Application of High-Energy Photon Beam to Industrial Imaging Based on Positron Annihilation

Hiroyuki Toyokawa[1], Tetsuya Hirade[2], Ryunosuke Kuroda[1], Ryoichi Suzuki[1], Toshiyuki Ohdaira[1]

[1]*National Institute of Advanced Industrial Science and Technology: 1-1-1 Umezono, Tsukuba, Ibaraki 3058568, Japan.*
h.toyokawa@aist.go.jp
[2]*Japan Atomic Energy Agency, 2-4 Shirane Shirakata, Tokai-mura, Naka-gun, Ibaraki 319-1195, Japan*

A novel method for industrial tomography based on positron annihilation has been presented. It is based on the 1st generation computed tomography, which uses high-energy photon beam produced via the laser-Compton scattering and 511 keV annihilation photons produced inside a testing object by the photon beam. Overall CT system, together with experimental results is described.

I. Introduction

Radiography is one of the most important and useful methods for nondestructive testing (NDT) of industrial products. Many radiography systems use bremsstrahlung x-rays from an x-ray tube, which emits x-rays about a few tens of keV.

Recently, an industrial computed tomography (CT) system using a high-energy and quasi-monochromatic photon beam has been developed[1]. The photon beam was generated via the laser-Compton scattering [2, 3]. Because the photon energy for the radiography system is typically 5 – 20 MeV with a few % energy spread, it scans large industrial products with very good density (low-contrast) resolution. The CT is based on the 1st generation method, which uses a narrowly collimated photon beam and a single photon detector. The testing object is placed on a CT stage, which translates, rotates, and elevates with respect to the photon beam.

When high-energy photons, typically 1 MeV or higher are incident on matter, primary interactions are the Compton scattering and the pair creation. Because the transmission CT uses only the transmitted photons, the information on the scattered photons and the annihilation photons was not necessary, and is discarded.

However, the information is very important because the distribution of the atomic numbers and the atomic or the electron densities can be estimated. In that sense, the present method is similar to the dual-energy CT [4].

In this paper, we describe the novel positron emission CT method using the laser-Compton photons in the MeV region, and demonstrated the dual-energy CT for NDT. The experimental setup is almost the same for the conventional 1st generation transmission CT experiment, except that an annihilation photon detector is placed adjacent to the testing object.

II. Laser-Compton photon beam

The laser-Compton photon is ideal for the industrial radiography for NDT. A high-energy, quasi-monochromatic photon beam with small angular spread in small beam diameter is generated with a simple method. We need an electron accelerator, an intense laser and some optical elements to generate the laser-Compton photons.

Eq. (1) tells us how to generate high-energy and quasi-monochromatic photon beam via laser-Compton scattering

$$E_\gamma = \frac{E_0(1-\beta\cos\theta_1)}{1-\beta\cos\theta_2 + E_0\dfrac{1-\cos(\theta_2-\theta_1)}{E_e}}, \quad (1)$$

where E_γ, E_0, E_e are the energies of the laser-Compton photons, laser photons and electrons. β, θ_1 and θ_2 are the velocity ratio of the electron to the light, angles of the direction of motion of an electron to a laser photon, and of an electron to a laser-Compton photon, respectively. A schematic drawing that shows the kinematics is shown in Fig. 1.

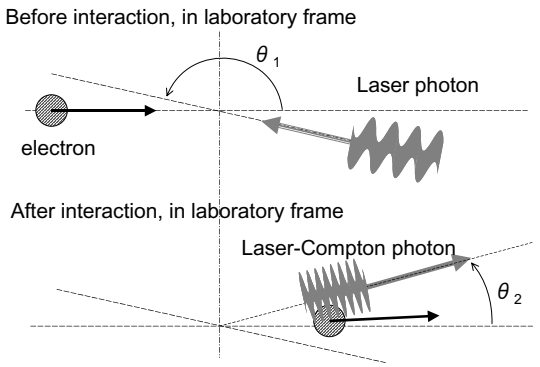

Fig. 1. Kinematics of the laser-Compton scattering.

III. Description of the CT method

A schematic drawing of the experimental setup for CT is shown in Fig. 2. The laser beam is focused on the electron beam, which counter-propagates to the laser beam. We used the electron storage ring TERAS [5] of AIST as the electron source. The laser beam collides head-on with the electron beam, and the back-scattered laser photons gained their energy from the electrons. We used 717.5 MeV electrons and 1064 nm laser light to generate 9.05 MeV laser-Compton photons.

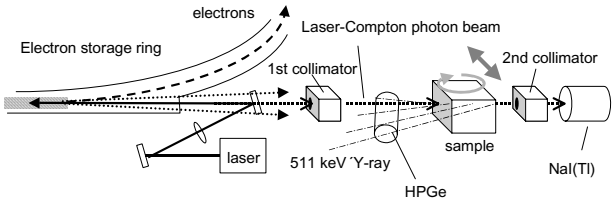

Fig. 2. Schematic view of the experimental setup for the CT experiments using the laser-Compton photons and the positron annihilation photons.

A lead block with a hole of 2 mm in diameter was aligned to the photon beam axis, which reduced the energy spread of the photons to a few %. It spatially shapes the transverse profile of the photon beam, too. The photons after the collimator were guided to the testing object, which was put on the CT stage. The beam size at the testing object is estimated to be about 4 mm, and the spatial resolution is about the same.

A horizontal view of the CT beamline is shown in Fig. 3. Transmitted photons through the testing object were collimated again with a lead collimator with a hole of 5 mm in diameter, and are detected by the NaI (Tl) scintillation counter (Scionix, 8"x12" single crystal with four PMTs). A high-purity germanium detector (EG&G ORTEC, model GEM-120225-P, HPGe hereafter) was placed in front of the testing object, out of the beam axis. It detects annihilation photons, which were produced along the passage of the photon beam in the testing object.

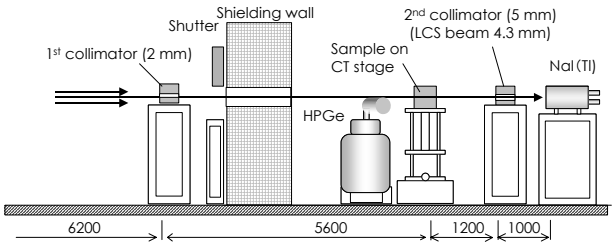

Fig. 3. Horizontal view of the laser-Compton CT beamline.

The raw data directly obtained from the experiment are the count-rates of the detectors at a certain location and angle of the testing object with respect to the photon beam. By normalizing the count-rates, we estimate the photon attenuation or the transmission. This quantity is an integrated value along the photon passage, and any integrals related to the testing object location and angle can be used for the CT data.

Because we measure the photon transmission one location by one using a single photon beam, total numbers of the annihilation photons produced along the beam axis can be such an integral. In this scheme, we can obtain two different CT images in a single run: one for the transmission and the other for the positron emission. Both measurements can be done independently and non-invasively to each other.

IV. Experiments

Figure 4 shows a block diagram for the present CT system. A two-channel counter/ scaler accumulates TTL pulses from a timing single channel analyzer (TSCA, EG&G ORTEC, model 420A) whose windows were set 7.5 – 10 MeV and 495 – 535 keV for NaI (Tl) and HPGe, respectively. The PC reads event numbers for the counter/ scaler every 1 mm, so that they correspond to the CT stage position.

When we need to measure the pulse height spectrum, signals from the pre-amplifier (PA) and the linear amplifier (LA, EG&G ORTEC, model 572A) are fed into the multi channel analyzer (MCA) with an appropriate delay via the delay amplifier (EG&G ORTEC, model 472A). The MCA only accepts linear pulses at the presence of the coincidence gate signal, which is generated via the gate and delay generator (EG&G ORTEC, model 416A) triggered by the TTL pulses.

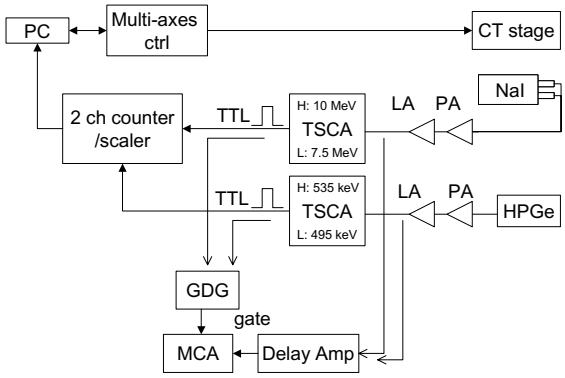

Fig. 4. Block diagram for the present CT system. TSCA (timing single channel analyzer). PA (pre-ampifier), LA (linear amplifier), MCA (multi channel analyzer), and GDG (gate and delay generator).

V. Experimental results

Figure 5 shows the pulse height spectra for the NaI(Tl) detector with and without the coincidence gate. Only the coincident events with the TSCA gate signal were included for the transmission CT data. Figures 6 show the pulse height spectra for the HPGe for (a) testing object was off-axis and the laser was off (blank), (b) testing object was on-axis but the laser was off, and (c) testing object was on-axis and the laser was on. When the laser turned on, the annihilation photons increased significantly. These spectra were taken for 3 min without the coincidence gate.

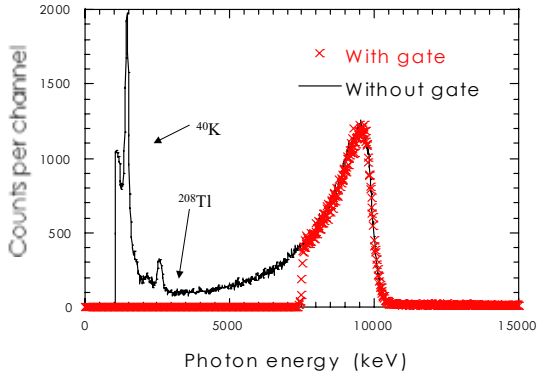

Fig. 5. Pulse height spectra of the NaI(Tl) detector with and without the coincidence gate. Two peaks at low energies are natural background gamma-rays from ^{40}K (1460.8 keV) and ^{208}Tl (2614.5 keV).

Figure 7 shows the pulse height spectra for the HPGe around 511 keV. The circles indicate the background annihilation photons from the testing object produced by the bremsstrahlung photons from the residual gas molecules in the storage ring. The squares are the foreground events when the laser was turned on and set to 10 W. The gates were off for the background and on for the foreground. The ratio of the background events to the foreground ones was 8%.

The annihilation photon peak was analyzed in detail. Figure 8 shows the peak spectrum for 511 keV gamma-rays together with the Gaussian fit curves. The peak was well described with two Gaussian curves with the spectrum widths of 3.70 keV and 7.12 keV in standard deviation. It is interesting that we can see the distribution of defects in material using the present method, in principle.

Figure 9 is the photograph of the testing object. It is a reinforced concrete block cut to 10 cm x 10 cm x 10 cm. Four reinforcement bars of different diameters are inserted perpendicular to the top face. CT-scanned layer was 2 cm under the top face. The broken circles on the photograph indicated the location of reinforcement bars.

Figure 10 show the CT images for the positron emission (left) and the transmission of laser-Compton photon (right), respectively. Image reconstruction was done with the filtered back-projection (FBP) method with Shepp-Logan filter and the Butterworth filter at the cut-off frequency (Nyquist frequency).

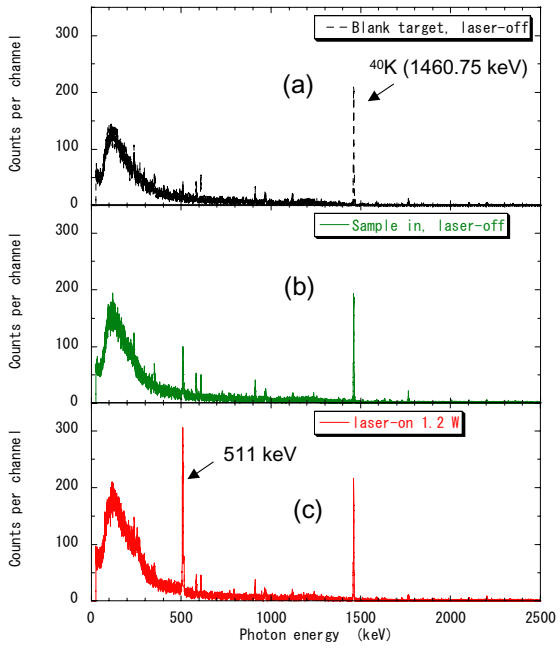

Fig. 6. Pulse height spectra of the HPGe for (a) testing object was off-axis and the laser was off (blank), (b) testing object was on-axis but the laser was off, and (c) testing object was on-axis and the laser was on. Coincidence gate was off.

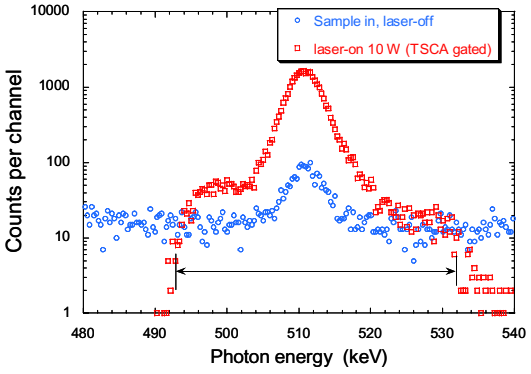

Fig. 7. Pulse height spectra for the HPGe around 511 keV.

Although we applied the photon counting method, the intensity of the annihilation photons was very low (100 Hz at max). So, the CT image for the positron

emission was a little noisy. However, reinforcement bars are clearly distinguished in both CT images.

VI. Discussion

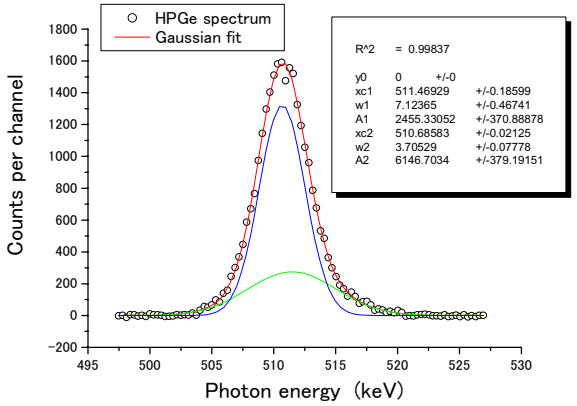

Fig. 8. Pulse height spectra of the HPGe detector for the annihilation photons together with the Gaussian fit curves. The spectrum was well described with two Gaussian curves with the spectrum widths of 3.70 keV and 7.12 keV in standard deviation.

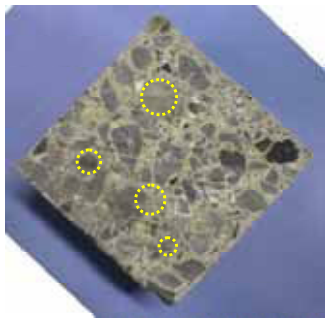

Fig. 9. Photograph of the testing object.

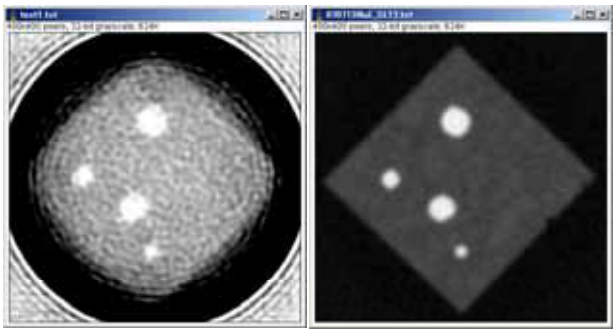

511 keV 9.05MeV

Fig. 10. CT images with the annihilation photons (left) and transmitted photons (right), respectively. Image reconstruction was done with the filtered back-projection (FBP) method with Shepp-Logan filter and the Butterworth filter at the cut-off frequency (Nyquist frequency).

There are several issues for the present method to be studied further. One of them is the background subtraction. The line-integral or the event numbers in i^{th} testing object location N_i is directly measured from the experiment. Background count N_i^b is estimated from the data analysis, which was subtracted from N_i. Then, they are normalized to the incident photons N_i^0 to give the photon attenuation or the product of the attenuation coefficient and the density, μ_i. Eq. (2) relates these parameters as

$$\mu_i = -\ln\left(\frac{N_i - N_i^b}{N_i^0}\right). \quad (2)$$

If N_i and N_i^b are very small, typically a few to a few tens, the error propagation formulae shown in Eqs. (3) ~ (5) tell us that the error of the photon attenuation coefficient, $\Delta\mu_i$ can be extremely large,

$$\Delta\mu_i = \sqrt{\left(\frac{\partial\mu_i}{\partial N_i}\Delta N_i\right)^2 + \left(\frac{\partial\mu_i}{\partial N_i^b}\Delta N_i^b\right)^2 + \left(\frac{\partial\mu_i}{\partial N_i^0}\Delta N_i^0\right)^2} \quad (3)$$

$$= \sqrt{\left(\frac{-\Delta N_i}{N_i - N_i^b}\right)^2 + \left(\frac{-\Delta N_i^b}{N_i - N_i^b}\right)^2 + \left(\frac{\Delta N_i^0}{N_i^0}\right)^2} \quad (4)$$

$$= \sqrt{\frac{(\Delta N_i)^2 + (\Delta N_i^b)^2}{(N_i - N_i^b)^2} + \left(\frac{\Delta N_i^0}{N_i^0}\right)^2}, \quad (5)$$

where ΔN_i, ΔN_i^b, ΔN_i^0 are the errors of N_i, N_i^b and N_i^0, respectively. The first term in the square root of Eq. (5) might be huge because the denominator sometimes nearly equals zero.

Another issue is an artifact caused by imperfect collection of annihilation photons. Cupping artifact was seen on the reconstructed CT image for 511 keV (Fig. 10 left). We should increase the number of detectors to make the testing object see them in 4π directions to suppress the artifact. It may be a good plan to introduce a correction factor based on analytical model or the Monte Carlo simulation for the image reconstruction process to compensate the imperfect collection of the annihilation photons. Further discussion about this issue is being undergone.

The present method is similar to the conventional dual-energy x-ray CT, but different in that it does not require multiple measurements. A single measurement using two detectors, one for the high-energy transmission photons and the other for the annihilation photons, was required. Signals from both detectors are processed independently to reconstruct CT images, but the geometry for both images was kept unchanged. The present method is free from the misalignment of the testing object.

A detailed analysis tells us that we can estimate the distributions of the atomic number and the atomic density with the present experiment. However, it is somewhat complicated, and requires much more space to describe. So, it will be discussed in the next paper.

VII. CONCLUSIONS

The novel CT method for industrial NDT, which introduced the positron emission CT into the 1st generation transmission CT using high-energy photon beam, has been presented. With the present method, two different CT images were obtained with a single measurement using photons of 9.05 MeV and 511 keV, respectively. Overall system was simple and similar to the conventional 1st generation transmission CT system using high-energy photon beam.

The transmission intensity of the 9.05 MeV photons was measured with the large NaI(Tl) scintillation detector to compute the transmission CT image. The 511 keV annihilation photons were created along the passage of the 9.05 MeV photon beam through the testing object, and the intensity was measured with the HPGe placed in front of the testing object to compute the positron emission CT image. So, both CT images had exactly the same spatial alignments of the testing object to the photon beam, and were free from misalignment.

Dual-energy CT with photons of large energy difference like the present method is effective for material recognition. However, the method is not straightforward to carry out because the primary interaction processes to the matters of 511 keV photons are the Compton scattering while those of 9.05 MeV photons are the Compton scattering and the pair creation. The analytical method is being studied, and the result will be presented soon.

In conclusion, we proposed the novel method to improve the quality of information for NDT using transmission CT by adding the information about the positron annihilation.

ACKNOWLEDGMENTS

This study was financially supported by the Budget for Nuclear Research of the Ministry of Education, Culture, Sports, Science and Technology of Japan, based on the screening and counseling by the Atomic Energy Commission of Japan.

REFERENCES

1. H. Toyokawa, H. Ogawa, H. Ohgaki, N. Aoki, N. Kobayashi, R. Kuroda, T. Kaihori and K. Yamada: *Proc. 5th International Symposium on Measurement Techniques for Multiphase Flows* (2006) 960-964.
2. H. Ohgaki, H. Toyokawa, K. Kudo, N. Takeda, and T. Yamazaki, *Nucl. Instrm. and Meth. in Phys. Res*. **A455**, 54-59 (2000).
3. R. H. Milburn, *Phys. Rev. Lett*. 10(3) 75-77 (1963).
4. R. E. Alvarez and A. Macovski, “Energy-selective Reconstructions in X-ray Computerized Tomography”, *Phys. Med. Biol.*, **21**, 733 (1976).
5. T. Tomimasu, T. Noguchi, S. Sugiyama, T. Yamazaki, and T. Mikado, "An Electron Undulating Ring for VLSI Lithography", *IEEE Trans. Nucl. Sci.*, **32**[5], 3403 (1985).